ELSEVIER

Journal of Membrane Science 116 (1996) 229–241

journal of MEMBRANE SCIENCE

Effects of natural convection instability on membrane performance in dead-end and cross-flow ultrafiltration

Kyung Ho Youm [a,*], Anthony G. Fane [b], Dianne E. Wiley [b]

[a] *School of Chemical Engineering, Chungbuk National University, Cheongju 361-763, Chungbuk, South Korea*

[b] *UNESCO Centre for Membrane Science and Technology, School of Chemical Engineering and Industrial Chemistry, University of New South Wales, Sydney, NSW, Australia, 2052*

Received 19 July 1995; accepted 30 January 1996

Abstract

The effects of natural convection instability on ultrafiltration performance have been tested experimentally in empty (without spacer) and spacer-filled channel cells. In dead-end operation, the permeate fluxes at the gravitationally unstable orientation of the empty cell are enhanced up to 3.5 times for dextran solution and 5.5 times for BSA solution compared with the results at the stable orientation. In cross-flow operation, flux improvement by natural convection instability occurs when the cross-flow velocity is below the critical value of around 0.1–0.2 m/s ($Re = 35$–90). A general criterion for determining whether natural convection effects dominate is identified considering the mass transfer between the membrane surface and the bulk. The criterion is that when $Gr/Re^2 >$ ca. 3 (for the empty cell) or $Gr/Re^2 >$ ca. 500 (for the spacer-filled cell) natural convection instability is of importance. A mass transfer correlation for the mixed convection membrane system is presented.

Keywords: Ultrafiltration; Concentration polarisation; Depolarisation; Natural convection instability; Mixed convection

1. Introduction

An inevitable feature of membrane processing is concentration polarisation which is a result of the accumulation of retained solutes at the membrane surface. In ultrafiltration (UF), this accumulation can lead to fouling due to the irreversible deposition of macromolecules both at the membrane surface and in the membrane pores. Concentration polarisation and fouling may result in a change in the membrane performance, i.e. a significant flux decline and an alteration of membrane retention.

To reduce or control concentration polarisation and fouling, many possible methods have been considered [1]. These are: (1) feed pretreatment, (2) modification of surface characteristics of the membrane, (3) providing good fluid management such as increasing shear at the membrane surface by increasing cross-flow velocity or producing eddies by using turbulence promoters, (4) regular chemical or mechanical cleaning of the membrane surface.

* Corresponding author. Tel.: +82 (431) 61-2491, FAX: +82 (431) 62-2380.

PII S0376-7388(96)00047-6

One of the most effective approaches for providing good fluid management is to induce fluid instability near the membrane surface by using pulsatile flow [2,3], and Taylor [4] and Dean [5,6] vortex flows. Winzeler and Belfort [6] have comprehensively reviewed several possible attempts to use fluid instabilities for improved membrane performance.

Another method capable of inducing fluid instability near the membrane surface is the use of natural convection. The variation of solute concentration across the concentration polarisation layer implies the existence of density variation so that the solution density at the membrane surface is higher than that in the bulk solution. By changing the gravitational orientation (angle) of the membrane module, the density inversion in which higher-density solutions overlay lower-density solutions is obtained. This density inversion may lead to unstable fluid behaviour and produce "natural convection (buoyancy or secondary) flow" in the vicinity of the membrane surface. The occurrence of natural convection may be effective to reduce concentration polarisation and fouling because of its effects in promoting mass transfer from the membrane surface to the bulk solution. Furthermore, if this natural convection is superimposed on the cross-flow (forced convective flow), it may be expected that the membrane performance will be significantly improved.

Natural convection has similar effects to other unstable flows such as Taylor vortices, Dean vortices and pulsatile flow but does not require the construction of a new design of membrane module. It is enough to simply change the gravitational orientation of existing flat membrane modules to obtain the effects of natural convection instability. It should also be noted that several conventional modules incorporate membrane surfaces at different orientations. For example a spiral-wound element aligned horizontally has membrane surfaces facing upward, downward and any angle in between. Performance correlations, such as those of Da Costa et al. [7], are typically obtained in flat-sheet simulators with the membrane at the bottom of the channel. The question arises as to whether those correlations are representative of modules having cylindrical (as for the spiral-wound element) geometry. It should be possible to identify the condition at which simulator results fail to be representative.

Some researchers have shown that the use of natural convection is effective to reduce or control concentration polarisation. Hendricks et al. [8] reported experimental observations for the existence of natural convection by using shadowgraph techniques and electrical conductivity microprobes in a dead-end and a cross-flow RO cell with a membrane at the upper wall of the cell. From these observations, they found that natural convection (they called it "convection-jet") occurred in a very narrow layer (around 300 μm) near the membrane surface and suggested that natural convection could be effective to reduce concentration polarisation both for laminar and turbulent regimes of the main flow (cross-flow). Huffman et al. [9] obtained, in cross-flow UF of 5% BSA and whole blood solutions, flux enhancement up to 200% when the membrane module was oriented to induce natural convection, and they interpreted this flux enhancement using the principles of heat transfer in the presence of natural convection. Slezak et al. [10] showed that the osmotic diffusion flux was significantly higher when the denser liquid was located above and the lighter liquid below the membrane in a horizontally mounted diffusion cell. They explained this observation in terms of natural convection instability that reduced boundary layer thickness.

This paper aims to obtain some information concerning the effects of natural convection instability on depolarisation and mass transfer in UF membrane systems. Thus, we focus on the effects of natural convection, with change of the membrane gravitational orientation, on the UF performance of relatively non-fouling solutes in the flat channel test cell operated in both the dead-end and the cross-flow modes. Most experiments were carried out in an empty (without spacer) cell. However a spacer-filled cell used previously as a spiral-wound "simulator" [7] was tested in the cross-flow mode. Defouling effects of natural convection instability are being tested and will be discussed in a future publication.

Using a direct analogy between heat and mass transfer, a criterion for determining whether natural convection instability is likely to affect the flux enhancement in cross-flow operation is identified. A mass transfer correlation, suitable for the combined natural and forced convection (mixed convection) membrane system, is presented and discussed.

2. Theory

2.1. Criterion for relative influence of natural and forced convection on membrane performance

In a manner similar to that used for analysing mixed convection heat transfer, an order-of-magnitude analysis of the boundary layer equation can be used to indicate the relative magnitudes of natural and forced convection effects in the membrane system [11].

Consider a pressurised feed solution which is pumped in laminar flow into a rectangular channel of channel height h, with the UF membrane attached at the upper wall surface. A description of the problem and the co-ordinate system are given in Fig. 1. Taking the flow in the direction of the feed solution as the x co-ordinate and the flow in the direction of the permeate as the y co-ordinate, the equation of motion in the y-direction for constant physical properties but variable density is:

$$U\frac{\partial J}{\partial x} = \nu\frac{\partial^2 J}{\partial x^2} + g\left(\frac{\rho-\rho_o}{\rho_o}\right) \tag{1}$$

The physical properties are calculated at the log-mean concentration between the bulk solution and the membrane surface. The last term on the right-hand side of Eq. (1) accounts for the buoyancy force induced by the density variation. The density variation may be expressed in terms of the volume expansion coefficient $\alpha[=(\partial\rho/\partial C)/\rho=(\Delta\rho/\Delta C)/\rho_o]$ induced by concentration difference and the concentration gradient $\beta[=\partial C/\partial y=\Delta C/\Delta y]$, so that we obtain

$$U\frac{\partial J}{\partial x} = \nu\frac{\partial^2 J}{\partial x^2} + g\alpha\beta y \tag{2}$$

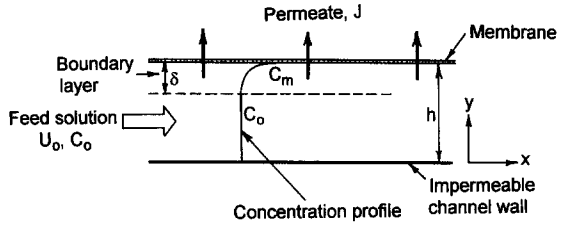

Fig. 1. Representation of concentration polarisation for membrane above the flow channel, i.e. at 180° cell orientation.

The following dimensionless quantities can be defined:

$$U^+=\frac{U}{U_o},\quad J^+=\frac{J}{U_o},\quad x^+=\frac{x}{h},\quad y^+=\frac{y}{h} \tag{3}$$

Eq. (2) becomes

$$U^+\frac{\partial J^+}{\partial x^+} = \frac{\nu}{U_o h}\frac{\partial^2 J^+}{\partial x^{+2}} + \frac{g\alpha\beta h^4}{\nu^2}\frac{\nu^2}{U_o^2 h^2}y^+ \tag{4}$$

Over the boundary layer of thickness δ, the left-hand side of Eq. (4) is of order of δ/h. On the right-hand side the viscous force and momentum transport are of the same order of magnitude, therefore the first (viscous) term is also of order of δ/h. Since y^+ is of the order of δ/h, the buoyancy term will be of importance if the coefficient of y^+ is of the order of 1 or greater [11,12]:

$$\frac{g\alpha\beta h^4}{\nu^2}\frac{\nu^2}{U_o^2 h^2} = 4\frac{Gr}{Re^2} \geq \text{order of 1} \tag{5}$$

where $Re\ (=U_o d_h/\nu)$ is the Reynolds number based on the hydraulic diameter d_h (for the thin-flat channel $d_h \approx 2h$) and $Gr\ (=g\alpha\beta h^4/\nu^2)$ is the Grashof number based on the concentration gradient. In the membrane system, Gr can be written appropriately as

$$Gr = \frac{g\alpha\beta h^4}{\nu^2} = \frac{g\alpha h^4 J C_{lm}}{\nu^2 D} \tag{6}$$

based on the assumption that $\beta = \mathrm{d}C/\mathrm{d}y$, so $D\beta = J\bar{C}$ at steady-state, and $\bar{C} = C_{lm}$, the log-mean concentration between the bulk solution and the membrane surface.

In a qualitative way the ratio Gr/Re^2 is an indication of the relative effects of natural and forced convection on the membrane module performance. A large Re implies a larger forced flow, and hence less influence of natural convection on module performance. A large Gr indicates a large concentration gradient in the boundary layer, and hence a larger effect of natural convection on module performance.

3. Experimental

The UF cell was a thin-channel type with an effective membrane area 50.75 cm^2 (active length

20.3 cm × width 2.5 cm, $h = 1.7 \times 10^{-3}$ m, $d_h = 3.18 \times 10^{-3}$ m, aspect ratio [height/width] = 6.8×10^{-2}). The inlet and outlet of this cell were connected to a piping system by means of couplings, which could provide easy rotation of the test cell. Details of the test cell and the experimental set-up were given by Da Costa et al. [7].

The membrane used was a HFK-131 polysulfone membrane with a nominal molecular weight cut-off of 5000 Da, supplied by Koch Membranes Inc. Before each run, the new membrane was soaked in a 30% ethanol solution for 30 min to remove glycerol from the pores and then was rinsed with ultrapure water several times.

In most experiments dextran 500T (average molecular weight 526 000, Sigma Co.) was used as a test solute at concentrations ranging from 1 to 10 kg/m^3. Bovine serum albumin (BSA, average molecular weight 68 000, Fraction V, Calbiochem Co.), dissolved in salt free ultrapure water (pH ≈ 5, $C_o = 1$ and 10 kg/m^3), was also used as a test solute for the dead-end UF experiments. Dextran concentrations in the feed and permeate were measured by the colorimetric method suggested by Dubois et al. [13], and BSA concentrations were analysed using the modified Lowry method [14]. The rejections (= [1 − permeate concentration/feed concentration] × 100) of dextran and BSA for the HFK-131 membrane were always larger than 99%.

The equations used for the density and viscosity of the dextran solutions as a function of concentration are:

$$\rho = 1013 + 0.33C \tag{7}$$

$$\mu = \exp(0.019C - 5.98) \tag{8}$$

The above relationships have been measured by Da Costa [15]. The other important properties of the dextran solution are osmotic pressure and diffusivity, which were given by Wijmans et al. [16] as:

$$\Delta\Pi = 8.67C + 0.298C^2 + 0.00898C^3 \tag{9}$$

$$D = \left(0.1204 + 2.614C_1 - 4.167C_1^2 + 2.132C_1^3\right) \times 10^{-10} \tag{10}$$

where $C_1 = C \times 10^{-3}$.

UF experiments were run using a horizontally aligned test cell, at three membrane gravitational cell orientations; the membrane surface was (1) below (gravitationally stable, designated 0°), (2) vertical to (semi-stable, 90°), (3) above (unstable, 180°) the flow channel. These orientations were obtained by simply rotating the test cell about its axis.

The effects of natural convection on the UF flux were examined in two operating modes; the dead-end and the cross-flow operation. In the dead-end operation, an empty (without spacer) cell was connected to a feed reservoir pressurised by nitrogen and permeates were recorded continuously by an electronic balance with an attached printer at 2-min intervals. The dead-end operation was performed at room temperature (≈ 20°C).

In the cross-flow operation, both an empty and spacer-filled cells were tested. One commercially available spacer designated as "80MIL-1" ($\theta = 80°$, $h = 2.03 \times 10^{-3}$ m, $\epsilon = 0.339$, $S_{vsp} = 3306$ m^{-1}, $d_h = 4.28 \times 10^{-4}$ m) was used. This spacer has already been characterised as a most effective spacer by Da Costa et al. [7,17]. In a typical cross-flow run, the initial membrane permeability was measured using pure water, and then the feed solution (about 8 l) was circulated at the required flow rate (varied from 3.4 to 124.7 l/h in the laminar regime), applied pressure (varied from 100 to 400 kPa) and at the specified cell orientation for about 20 min to allow stabilisation of temperature (25°C). Then the permeate flux was recorded at 1- or 2-min intervals for 20 or 30 min and the channel pressure drop was measured. All flux data for cross-flow UF reported here are the average values of 8 to 14 measurements with standard deviations ranging from 0.6 to 3%. A new set of operating conditions and cell orientation was then selected and measurements were repeated. After a series of runs the system was flushed with ultrapure water and the membrane permeability (as determined by pure water flux) was rechecked, but no decrease in the permeability was detected. The osmotic pressure and film models [18,19] were used to determine C_m, the concentration at the membrane surface, and k, the mass transfer coefficient:

$$J = L_p(\Delta P_{TM} - \Delta\Pi_m) \tag{11}$$

$$J = k\ln(C_m/C_o) \tag{12}$$

where ΔP_{TM} is the average transmembrane pressure calculated from the applied pressure ΔP and the channel pressure drop ΔP_{CH}, i.e. $\Delta P_{TM} = \Delta P - 0.5\Delta P_{CH}$.

4. Results and discussion

4.1. Dead-end UF

To show the magnitude of the effects of natural convection on the UF performance for dead-end operation, the UF of dextran and BSA solutions was performed (at 300 kPa) in an empty cell with change of the feed concentration. For each run, the time dependent fluxes were continuously recorded in four successive stages (each stage lasted for 30 min): (1) filtration at 0° cell orientation, followed by (2) cell orientation changed to 180° and filtration, then (3) cell orientation changed to 90° and filtration, finally (4) cell was reoriented to 0° and filtration.

The flux–time behaviours for dextran and BSA solutions during the four successive stages are shown in Figs. 2 and 3, respectively. During stage 1 (0°, gravitationally stable), the flux declines very rapidly in the first few minutes, due to the development of concentration polarisation, and then continues to decline until the cell orientation is changed to 180°. During stage 2 (180°, gravitationally unstable), the flux increases rapidly for 5 to 10 min, due to depolarisation, and then reaches the enhanced steady value. The flux enhancements are in the range around 1.5 to 3.5 times for dextran with change of the feed concentration and 2 to 5.5 times for BSA compared

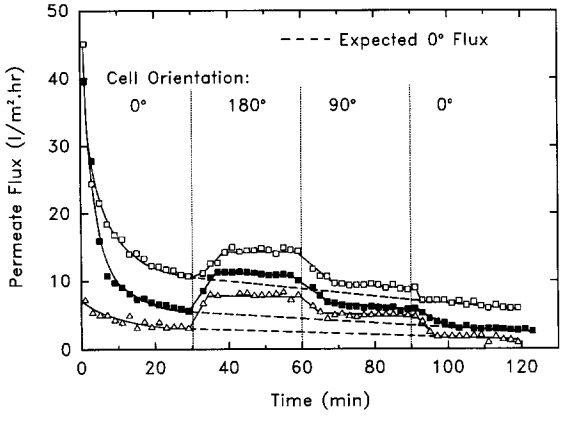

Fig. 2. Flux vs. time behaviour for dead-end UF of dextran solution during four successive changes of cell orientation in the empty cell at different feed concentrations [$\Delta P = 300$ kPa, (□); $C_0 = 1$ kg/m^3, (■); $C_0 = 5$ kg/m^3, (△); $C_0 = 10$ kg/m^3].

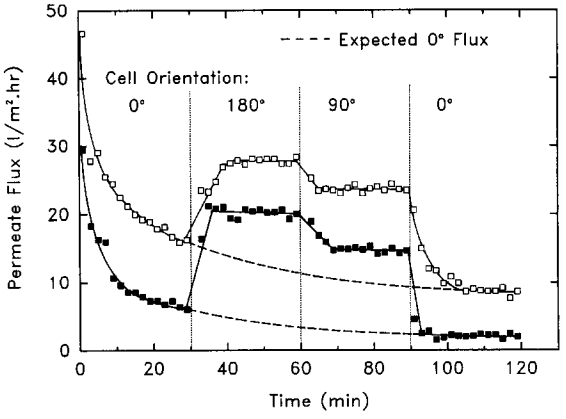

Fig. 3. Flux vs. time behaviour for dead-end UF of BSA solution during four successive changes of cell orientation in the empty cell at different feed concentrations [$\Delta P = 300$ kPa, pH = 5, (□); $C_0 = 1$ kg/m^3, (■); $C_0 = 10$ kg/m^3].

with the expected 0° flux lines (the regression lines of the flux data in stages 1 and 4, which are well confirmed by the following dead-end UF results; see Fig. 4a and Fig. 5a). These flux enhancements imply that natural convection flow induced by the density inversion produces a gravitationally unstable state in the concentration boundary layer and this instability may promote the movement of accumulated solutes away from the membrane surface (depolarising). In stage 3 (90°, gravitationally semi-stable), we also obtain enhanced steady values (the flux enhancements are around 1.2 to 2.5 times for dextran and 1.5 to 5 times for BSA) although these are less than flux obtained at 180°. The above results indicate that the maximum instability may be obtained when the density inversion is complete (i.e. at 180° orientation). During stage 4 (0°), the flux decreases rapidly in the first few minutes and then declines slowly reaching values similar to that obtained if the whole experiments were carried out at 0°. This implies that the flux is independent of the previous orientation history.

It is interesting to note that the enhanced values for BSA are higher than those for dextran and the enhanced flux does not decline over the time of these experiments (Fig. 3). We anticipate that this may be due to the defouling effects of natural convection instability. This factor will be the subject of a future paper.

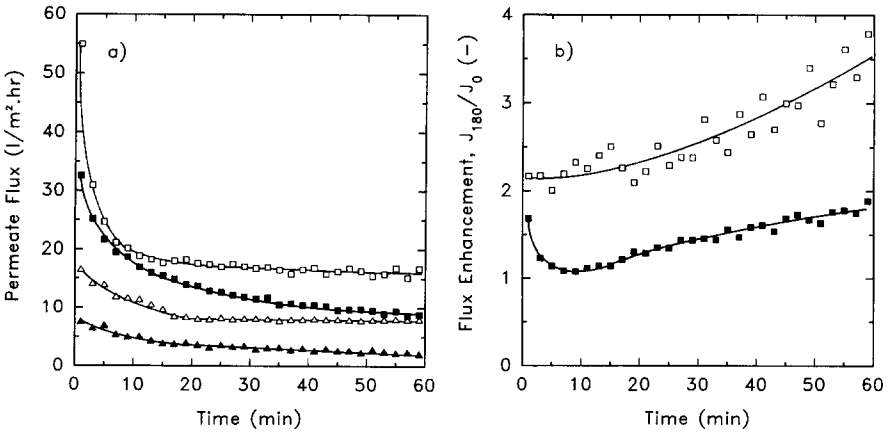

Fig. 4. (a) Flux trends at 0° and 180° cell orientations and (b) flux enhancement trends at 180° cell orientation for dead-end UF of dextran solution in the empty cell at different feed concentrations [$\Delta P = 300$ kPa, (a) (■); $C_0 = 1$ kg/m^3, 0°, (□); $C_0 = 1$ kg/m^3, 180°, (▲); $C_0 = 10$ kg/m^3, 0°, (△); $C_0 = 10$ kg/m^3, 180°, (b) (■); $C_0 = 1$ kg/m^3, (□); $C_0 = 10$ kg/m^3].

Another set of dead-end UF experiments for dextran solutions was carried out to measure quantitatively the depolarising effects of natural convection instability. Experiments were only executed at stable (0°) and unstable (180°) orientations. Flux and flux enhancement (flux ratio = J_{180}/J_0) with time under various experimental conditions are shown in Figs. 4 and 5. Fig. 4 shows the influence of feed concentration, while Fig. 5 shows the influence of applied pressure.

The flux trends for 0° and 180° cell orientation are somewhat different (Fig. 4a and Fig. 5a). After the initial rapid drop, the flux decreases slowly with time for 0° cell orientation but it reaches a steady (enhanced) value for 180° cell orientation at all feed concentrations and pressures. The difference may be attributed to the boundary layer disturbance at 180° cell orientation, that is, the mass transfer is enhanced by natural convection instability. An estimate of the mass transfer coefficient k based on the film model supports this explanation. For example, in the case of $C_0 = 5$ kg/m^3 and $\Delta P = 300$ kPa, k values after the

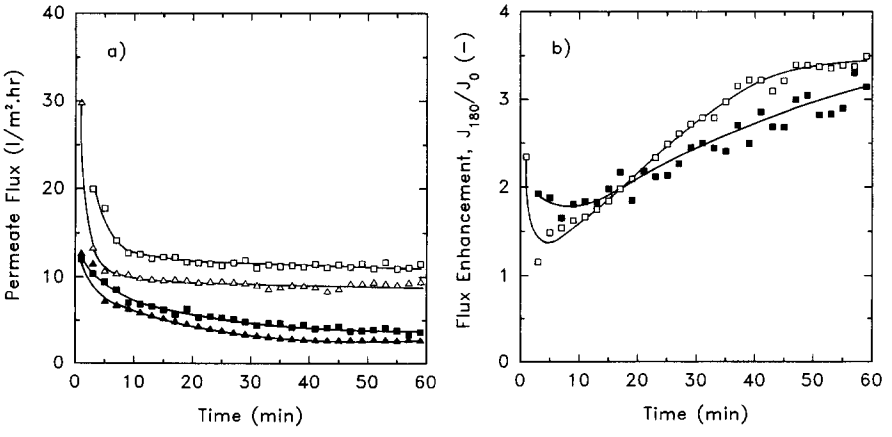

Fig. 5. (a) Flux trends at 0° and 180° cell orientations and (b) flux enhancement trends at 180° cell orientation for dead-end UF of dextran solution in the empty cell at different applied pressures [$C_0 = 5$ kg/m^3, (a) (▲); $\Delta P = 100$ kPa, 0°, (△); $\Delta P = 100$ kPa, 180°, (■); $\Delta P = 300$ kPa, 0°, (□); $\Delta P = 300$ kPa, 180°, (b) (□); $\Delta P = 100$ kPa, (■); $\Delta P = 300$ kPa].

initial rapid flux drop are almost constant at 7.6×10^{-7} m/s for 180° cell orientation while they decrease from 4.5×10^{-7} to 2.5×10^{-7} m/s for 0° cell orientation. These different flux trends lead to increase in flux enhancement with time except for the initial few minutes. Initial ambiguous trends may be caused by air remaining in the permeate side at the beginning of the measurements. A higher feed concentration gives a greater flux enhancement, thus, J_{180}/J_0 increases by a factor of up to 3.5 for $C_0 = 10$ kg/m^3, and by a factor of < 2.0 for $C_0 = 1$ kg/m^3 (Fig. 4b). However the applied pressure has almost no influence on the flux enhancement (Fig. 5b).

4.2. Cross-flow UF

4.2.1. Flux results

Cross-flow UF was carried out only for dextran solutions in an empty and a spacer-filled cell. First of all, to instantly determine the effects of natural convection on the UF performance in cross-flow operation, fluxes versus time (at $C_0 = 5$ kg/m^3 and $\Delta P = 300$ kPa) in an empty and a spacer-filled cell with accompanying successive changes of the cell orientation (0° → 180° → 90° → 0°) were measured for three different flow rates; 3.4 l/h, 19.5 l/h and 62.8 l/h. These results are illustrated in Fig. 6, where the time zero indicates the beginning of flux measurements after the solution temperature has stabilised. At 0° cell orientation, improved fluxes with the 80MIL-1 spacer-filled cell over the empty channel are clear with enhancements in the range 2.5 to 3 times, which are consistent with the data of Da Costa et al. [7].

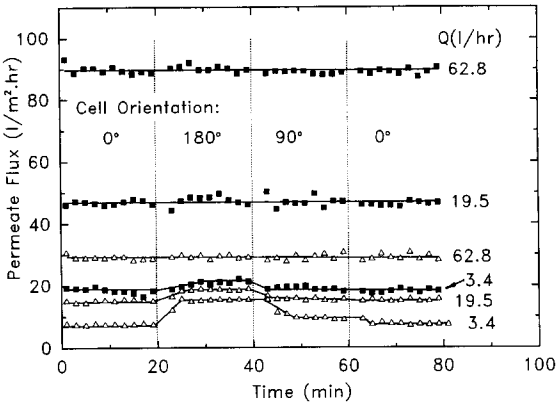

Fig. 6. Flux vs. time behaviour for cross-flow UF of dextran solution during four successive changes of cell orientation in the empty and 80MIL-1 spacer-filled cell at different cross-flow rates [$C_0 = 5$ kg/m^3, $\Delta P = 300$ kPa, (△); empty cell, (■); 80 MIL-1 spacer-filled cell].

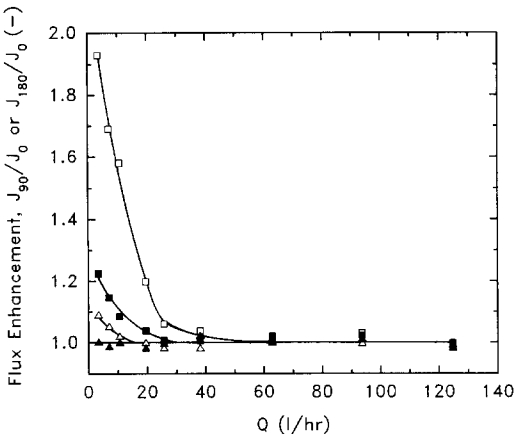

Fig. 7. Flux enhancements at 90° and 180° cell orientations for cross-flow UF of dextran solution in the empty and 80MIL-1 spacer-filled cell as a function of cross-flow rate [$C_0 = 5$ kg/m^3, $\Delta P = 300$ kPa, (■); empty cell, 0°, (□); empty cell, 180°, (▲); 80 MIL-1 spacer-filled cell, 0°, (△); 80 MIL-1 spacer-filled cell, 180°].

Flux enhancements by natural convection at 180° cell orientation are also observed for cross-flow UF in the empty channel (1.95 times at 3.4 l/h and 1.20 times at 19.5 l/h) although they are lower than those obtained for the dead-end UF and are not evident at 62.8 l/h. Moreover flux enhancements are obtained only at 3.4 l/h for the 90° cell orientation of the empty channel (1.23 times) and the 180° cell orientation of the spacer-filled cell (1.12 times); no flux improvements are found at 90° cell orientation in the spacer-filled cell. Hence, it is evident that the cross-flow conditions, i.e. flow velocity and turbulence produced by spacers, are significant factors controlling the natural convection instability in the mixed convection membrane systems. To examine these factors more cross-flow runs were done with change in the operating conditions – especially emphasising the variation of flow rate. The cross-flow rate Q was varied from 3.4 to 124.7 l/h corresponding to a cross-flow velocity from 0.02 to 0.82 m/s (*Re* from 5 to 560) for the empty cell and from 0.06 to 2 m/s (*Re* from 2 to 180) for the spacer-filled cell.

The results are shown in Fig. 7 which indicates

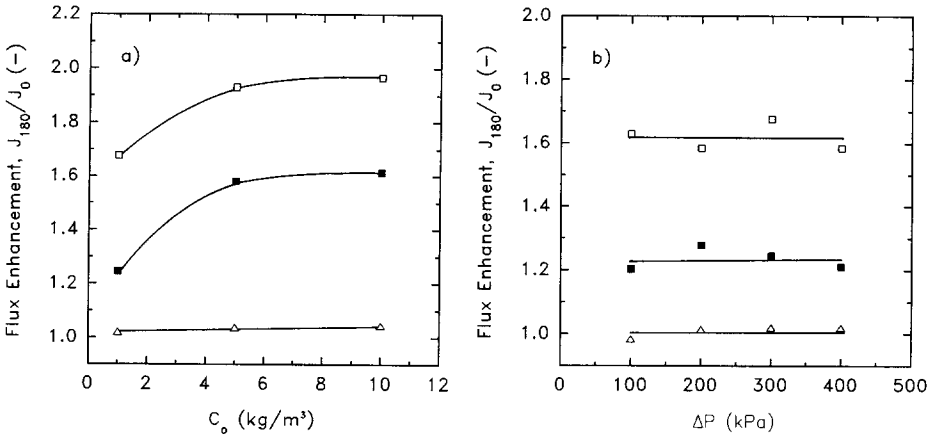

Fig. 8. Flux enhancements at 180° cell orientation for cross-flow UF of dextran solution in the empty cell as a function of (a) feed concentration and (b) applied pressure [(a) $\Delta P = 300$ kPa, (b) $C_0 = 1$ kg/m^3, (□); $Q = 3.4$ l/h, (■); $Q = 10.6$ l/h, (△); $Q = 38.1$ l/h].

that flux enhancements by natural convection are influenced significantly by the cross-flow rate and the presence of spacers. Fig. 8 shows that flux enhancements are more considerable for higher concentration (Fig. 8a), however the applied pressure does not affect flux enhancements (Fig. 8b) as found for dead-end UF (Fig. 5b). Typical cross-flow UF results are summarised in Table 1 for $C_0 = 10$ kg/m^3 and $\Delta P = 300$ kPa. The natural convection instability may be considered to be effective for UF performance if the flux improvement represents more than ca. 10%. Application of this 10% criterion to the results in Table 1 for the empty channel yields a critical cross-flow velocity of approximately 0.1–0.2

Table 1
Typical cross-flow UF experimental data at $C_0 = 10$ kg/m^3 and $\Delta P = 300$ kPa

Channel type	Q	ΔP_{CH} ($\times 10^{-3}$)	U_0	J ($\times 10^7$) (m/s)			Flux enhancement (–)	
	(l/h)	(Pa)	(m/s)	0°	90°	180°	J_{90}/J_0	J_{180}/J_0
Empty	3.4	0	0.02	16.2	18.8	31.8	1.16	1.96
(without spacer)	7.0	0	0.05	19.7	22.6	34.8	1.15	1.77
	10.6	0	0.07	23.3	25.4	37.6	1.09	1.61
	19.5	0.05	0.13	28.9	31.6	39.9	1.09	1.38
	25.7	0.12	0.17	38.6	37.9	42.8	0.98	1.10
	38.1	0.25	0.25	44.3	43.3	46.3	0.98	1.04
	62.8	0.40	0.41	56.2	55.9	56.4	0.99	1.01
	93.7	0.59	0.61	67.6	66.5	65.9	0.98	0.98
	124.7	0.77	0.82	75.1	77.7	74.5	1.03	0.99
80MIL-1	3.4	0.19	0.06	36.4	38.6	41.2	1.06	1.13
spacer-filled	7.0	0.49	0.11	51.7	53.9	54.2	1.04	1.05
	10.6	0.87	0.17	64.4	65.3	66.5	1.01	1.03
	19.5	1.73	0.32	84.9	85.3	85.7	1.00	1.01
	25.7	3.40	0.42	118.5	118.0	118.1	1.00	1.00
	38.1	5.87	0.61	142.3	143.9	138.0	1.01	0.97
	62.8	15.14	1.01	170.7	171.6	172.4	1.01	1.01
	93.7	29.66	1.51	203.1	197.0	201.2	0.97	0.99
	124.7	48.57	2.01	218.8	217.7	220.3	0.99	1.01

m/s. This critical cross-flow velocity can be compared with a critical velocity of around 0.3 m/s for mixed convection heat transfer [20]. For cross-flow velocities beyond the critical value it would be expected that forced convection would overshadow the effects of natural convection.

A brief description of the operating conditions for various commercial UF modules is given in Table 2. The critical cross-flow velocity of 0.1–0.2 m/s corresponds to a Re of 35–90. These values of Re are around the lower limit values of Re for all commercial UF modules except the tubular module. Thus, one can expect to achieve flux improvements of 10% or more due to natural convection instability for commercial UF modules if these modules are aligned to the gravitationally unstable orientation and are operated at low cross-flow rates. Furthermore, it should be pointed out that the operation of modules at low cross-flow rate has the following benefits in addition to the flux enhancement by natural convection instability; reduction in power consumption for pumping, low channel pressure drop and minimisation of the denaturation of shear-labile solutes.

4.2.2. Relative influence of natural and forced convection flows on mass transfer

To obtain a general criterion for determining whether natural convection effects dominate, the cross-flow UF results are represented in Fig. 9 as $(Sh_M - Sh_F)/Re$ as a function of Gr/Re^2. Sh_M and Sh_F are the Sherwood numbers for 90° or 180° cell orientation (mixed convection) and for 0° cell orientation (forced convection) respectively. $(Sh_M - Sh_F)/Re$ represents the net mass transfer by natural convection instability to the bulk solution of unit flow rate since Re is by definition the dimensionless flow rate [23].

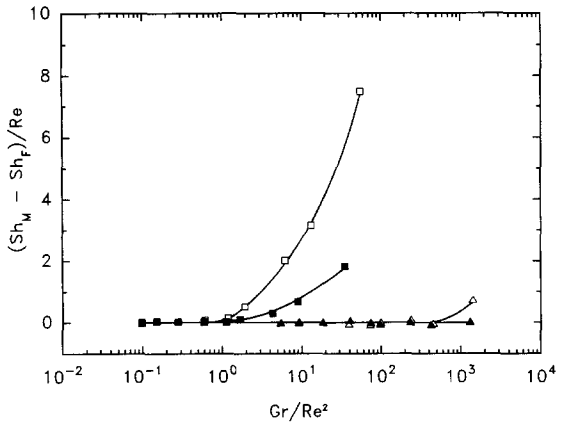

Fig. 9. Net mass transfer at 90° and 180° cell orientations with change of Gr/Re^2 for cross-flow UF of dextran solution in the empty and 80MIL-1 spacer-filled cell [$C_0 = 5$ kg/m^3, $\Delta P = 300$ kPa, (■); empty cell, 90°, (□); empty cell, 180°, (▲); 80 MIL-1 spacer-filled cell, 90°, (△); 80 MIL-1 spacer-filled cell, 180°].

Fig. 9 shows that the net mass transfer to the bulk solution of unit flow rate is nearly zero at small values of Gr/Re^2 where forced convection dominates, it increases with increasing Gr/Re^2 beyond a threshold value at which the mass transfer may be enhanced appreciably by natural convection instability. Fig. 9 also shows that the net mass transfer is

Table 2
Operating conditions for various commercial UF modules

Module	d_h or h (mm)	ΔP (10^5 Pa)	U_0 (m/s)	Re [c]
Hollow fiber [a]	0.5–2	< 2.5	0.5–3.5	10–1000 Laminar
Tubular [a]	10–25	3–25	2–6	10000–30000 Turbulent
Plate frame [a]	0.3–1	5–20	0.7–2	100–6000 Normally laminar
Spiral wound [b]	0.7–1.1	> 10	0.1–0.6 [d]	70–660 [d] Spacers induce turbulence

[a] Taken from Kulkarni et al. [21].
[b] Taken from Holeschovsky and Cooney [22].
[c] Values based on the hydraulic diameter d_h.
[d] Values based on the empty (without spacers) channels.

largest for the empty cell and the complete density inversion case (180° cell orientation). Here it is worth noting that the use of Gr/Re^2 is more suitable than the use of individual parameters such as cross-flow velocity or density difference for determining the relative influence of natural and forced convection effects on the membrane performance because Gr/Re^2 contains both the buoyancy and the forced convection terms. Gr/Re^2 characterises the dominant mode of mass transfer in mixed convection membrane systems.

The effects of the feed concentration and applied pressure on the net mass transfer are given in Fig. 10 for the empty cell at 180° cell orientation, which shows that a higher feed concentration provides a larger net mass transfer at the same Gr/Re^2 above the threshold value but variation in pressure hardly affects the net mass transfer. Noting the Schmidt numbers in Fig. 10, the increase of Sc with feed concentration is more considerable than that with pressure. Acrivos [24] and Churchill [25] showed that the Prandtl number for large values ($\gg 1$) also controlled the combined effects of natural and forced convection heat transfer. Thus, in the mixed convection membrane systems it might be expected that the Schmidt number Sc, in addition to Gr/Re^2, is an important parameter controlling the relative importance of natural and forced convection.

The threshold values of Gr/Re^2, defined as the value at which the flux improvement represents more than ca. 10%, for the empty and spacer-filled cells at 90° and 180° cell orientations are summarised in Table 3. These values are determined from regression lines of the data. The threshold values for the empty cell are lower than those for the spacer-filled cell and decrease with increasing feed concentration (increasing Sc). Based on the results in Table 3 natural convection instability may influence membrane performance when Gr/Re^2 has a value higher than around 3 for the empty cell and around 500 for the spacer-filled cell.

Table 3
Threshold values of Gr/Re^2

Channel type		Feed concentration (kg/m^3)		
		1	5	10
Empty	180°	3	1	0.9
	90°	8	3.4	2.3
80MIL-1	180°	720	405	247
	90° [a]			

[a] No natural convection instability effects are detected.

4.2.3. Mass transfer correlation for mixed convection membrane system

A mass transfer correlation for the mixed convection membrane systems was developed for the empty cell at 180° cell orientation which represents the

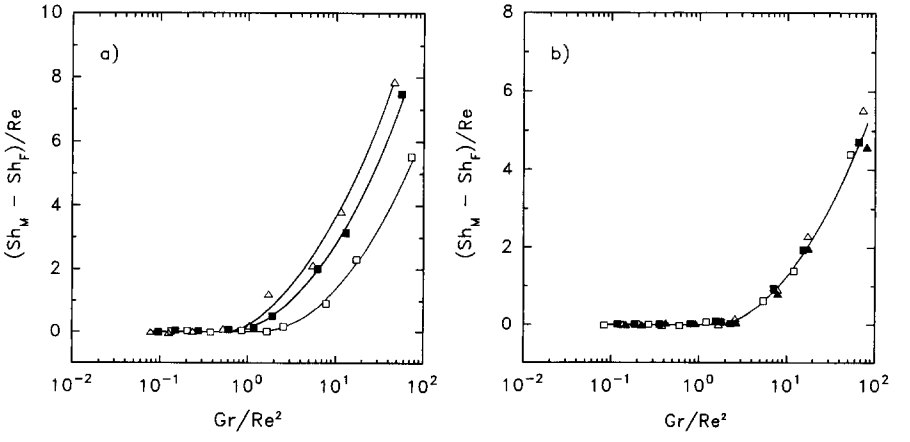

Fig. 10. Net mass transfer at 180° cell orientation with change of Gr/Re^2 for cross-flow UF of dextran solution in the empty cell as a function of (a) feed concentration and (b) applied pressure [(a) $\Delta P = 300$ kPa, (□); $C_0 = 1$ kg/m^3, $Sc = 2.70 \times 10^5$, (■); $C_0 = 5$ kg/m^3, $Sc = 3.35 \times 10^5$, (△); $C_0 = 10$ kg/m^3, $Sc = 3.96 \times 10^5$, (b) $C_0 = 1$ kg/m^3, (□); $\Delta P = 100$ kPa, $Sc = 2.34 \times 10^5$, (■); $\Delta P = 200$ kPa, $Sc = 2.53 \times 10^5$, (△); $\Delta P = 300$ kPa, $Sc = 2.70 \times 10^5$, (▲); $\Delta P = 400$ kPa, $Sc = 2.83 \times 10^5$].

highest mass transfer enhancement by natural convection instability and provides a significant amount of data.

Using a direct analogy between heat and mass transfer, we can write the Sherwood number for mixed convection Sh_M as follows [25]:

$$\frac{Sh_M}{Sh_F} = \left[1 + \left(f\{Sc\}Gr/Re^2\right)^{n/4}\right]^{1/n} \quad (13)$$

where Sh_F indicates the Sherwood number for pure forced convection ($Gr/Re^2 \to 0$), $f\{Sc\}$ is a function of the Schmidt number, i.e. $f\{Sc\} = aSc^b$, and n is an arbitrary power. The values of the constants a, b and n for Eq. (13) were determined by non-linear regression. The following equation was obtained from experimental data for all feed concentrations and applied pressures for the empty cell at 180° cell orientation.

$$\frac{Sh_M}{Sh_F} = \left[1 + 1.24\left(Gr/Sc^{0.143}Re^2\right)^{3/4}\right]^{1/3} \quad (14)$$

The power n of 3 is in general agreement with the value in the range from 2 to 4 for mixed convection heat transfer [25]. Eq. (14) fits the experimental data with a standard deviation of 15.6% (Fig. 11). This deviation is reasonable considering the usual large scatter in heat and mass transfer correlations. In addition the mass transfer correlation for the forced convection data of the empty cell (0° cell orientation) was obtained. The equation is:

$$Sh_F = 0.303Re^{0.465}Sc^{1/3} \quad (15)$$

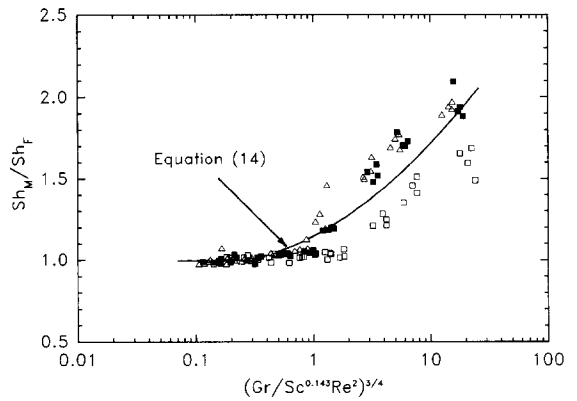

Fig. 11. Sh_M/Sh_F vs. $(Gr/Sc^{0.143}Re^2)^{3/4}$ plot for the empty cell at 180° cell orientation [(□); $C_o = 1$ kg/m^3, (■); $C_o = 5$ kg/m^3, (△); $C_o = 10$ kg/m^3].

The Reynolds number exponent of 0.465 is different from the usual value of 0.33 for laminar condition. This difference may be due to the entrance and exit effects of the "short" channel [7]. Thus we can rewrite Eq. (14) as follows:

$$Sh_M = 0.303Re^{0.465}Sc^{1/3} \times \left[1 + 1.24\left(Gr/Sc^{0.143}Re^2\right)^{3/4}\right]^{1/3} \quad (16)$$

5. Conclusions

UF experimental data obtained with a flat channel cell at various orientations with or without a spacer show that natural convection instability affects the membrane performance at the unstable gravitational orientation (membrane above the flow channel).

In dead-end operation, the permeate fluxes in the empty cell are enhanced up to 3.5 times for dextran solution and 5.5 times for BSA solution by natural convection instability.

In cross-flow operation, flux enhancements by natural convection are significantly influenced by the cross-flow rates; cross-flow velocities beyond the critical value of 0.1–0.2 m/s ($Re = 35$–90) may overshadow the effects of natural convection. Although the tests conducted were over a relatively short time frame the observed effects are likely to be sustained over much longer times since the natural convection will continue to produce disturbances indefinitely. We anticipate that if commercial UF modules are aligned to the unstable orientation and are operated at below the critical cross-flow velocity, flux enhancements of more than 10% should be obtained due to natural convection instability. However it should be noted that most commercial units tend to be operated above the critical cross-flow velocity. A corollary of this is that correlations based on flat channel simulators with spacers in the 0° cell orientation would be applicable to most applications of spiral-wound elements. A general criterion, which is that when $Gr/Re^2 >$ ca. 3 for the empty cell and $Gr/Re^2 >$ ca. 500 for the spacer-filled cell, for determining the relative influence of natural and forced convection on the membrane performance has been identified. Besides Gr/Re^2, the Schmidt number Sc

also controls the relative importance of natural and forced convection. Mass transfer in the mixed convection membrane system can be described by Eq. (14), which is similar in form to that used for analysing mixed convection heat transfer.

Further studies on the defouling effects of natural convection instability are required.

6. List of symbols

C	concentration (kg/m^3)
$\overline{C}$	average concentration over the boundary layer (kg/m^3)
C_{lm}	log-mean concentration between the bulk solution and the membrane surface (kg/m^3)
D	diffusion coefficient (m^2/s)
$d_h = 4\epsilon/[(2/h) + (1-\epsilon)S_{vsp}]$	hydraulic diameter (m)
$Gr = g\alpha\beta h^4/\nu^4$	Grashof number (–)
g	gravitational acceleration (m/s^2)
h	channel height or spacer thickness (m)
J	permeate flux (m/s)
$J^+ = J/U_o$	dimensionless permeate flux (–)
k	mass transfer coefficient (m/s)
L_p	membrane permeability (m/Pa s)
n	arbitrary power in Eq. (13) (–)
ΔP	applied pressure (Pa)
ΔP_{CH}	channel pressure drop (Pa)
ΔP_{TM}	transmembrane pressure (Pa)
Q	cross-flow rate (l/h)
$Re = U_o d_h/\nu$	Reynolds number (–)
$Sc = \nu/D$	Schmidt number (–)
$Sh = kd_h/D$	Sherwood number (–)
S_{vsp}	specific surface of spacer (m^{-1})
U	cross-flow velocity at any point in the channel (m/s)
$U_o = Q/(hw\epsilon)$	cross-flow velocity at entrance to the channel (m/s)
$U^+ = U/U_o$	dimensionless cross-flow velocity (–)
w	width (m)
x	x-direction length (m)
$x^+ = x/h$	dimensionless x-direction length (–)
y	y-direction length (m)
$y^+ = y/h$	dimensionless y-direction length (–)
$\alpha = (1/\rho)(\partial\rho/\partial C)$	volume expansion coefficient (m^3/kg)
$\beta = \partial C/\partial y$	concentration gradient (kg/m^4)
δ	boundary layer thickness (m)
ϵ	voidage of spacer (–)
θ	characteristic angle of spacer (°)
μ	viscosity (Pa s)
ν	kinematic viscosity (m^2/s)
$\Delta\Pi$	osmotic pressure difference (Pa)
ρ	density (kg/m^3)

6.1. subscripts

0	0° cell orientation
90	90° cell orientation
180	180° cell orientation
F	forced convection
M	mixed convection
o	bulk or feed
m	membrane surface

Acknowledgements

The authors wish to acknowledge the financial support of the Australian Research Council and the supply of membrane by Koch Membranes Inc. One of the authors (K.H. Youm) is supported by the Korea Science and Engineering Foundation (KOSEF), which is gratefully acknowledged.

References

[1] A.G. Fane and C.J.D. Fell, A review of fouling and fouling control in ultrafiltration, Desalination, 62 (1987) 117–136.

[2] V.G.J. Rodgers and R.E. Sparkes, Effect of transmembrane pressure pulsing on concentration polarization, J. Membrane Sci., 68 (1992) 149–168.
[3] C.D. Bertram, M.R. Hoogland, H. Li, R.A. Odell and A.G. Fane, Flux enhancement in crossflow microfiltration using a collapsible-tube pulsation generator, J. Membrane Sci., 84 (1993) 279–292.
[4] K.H. Kroner and V. Nissinen, Dynamic filtration of microbial suspensions using an axially rotating filter, J. Membrane Sci., 36 (1988) 85–100.
[5] K.Y. Chung, B. Bates and G. Belfort, Dean vortices with wall flux in a curved channel membrane system 4. Effect of vortices on permeation fluxes of suspensions in microporous membrane, J. Membrane Sci., 81 (1993) 139–150.
[6] H.B. Winzeler and G. Belfort, Enhanced performance for pressure-driven membrane processes: the argument for fluid instabilities, J. Membrane Sci., 80 (1993) 35–47.
[7] A.R. Da Costa, A.G. Fane, C.J.D. Fell and A.C.M. Franken, Optimal channel spacer design for ultrafiltration, J. Membrane Sci., 62 (1991) 275–291.
[8] T.J. Hendricks, J.F. Macquin and F.A. Williams, Observation on buoyant convection in reverse osmosis, Ind. Eng. Chem. Fundam., 11 (1972) 276–279.
[9] W.J. Huffman, R.M. Ward and R.C. Harshman, Effects of forced and natural convection during ultrafiltration of protein–saline solutions and whole blood in thin channels, Ind. Eng. Chem., Process Des. Dev., 14 (1975) 166–170.
[10] A. Slezak, K. Dworecki and J.E. Anderson, Gravitational effects on transmembrane flux: the Rayleigh–Taylor convective instability, J. Membrane Sci., 23 (1985) 71–81.
[11] B. Gebhart, Heat Transfer, 2nd edn. McGraw-Hill, New York, 1971, pp. 388–397.
[12] A. Bejan, Heat Transfer, Wiley, New York, 1993, pp. 231–239.
[13] M. Dubois, K.A. Gilles, J.K. Hamilton, P.A. Rebers and F. Smith, Colorimetric method for determination of sugars and related substances, Anal. Chem., 28 (1956) 350–356.
[14] H.H. Hess, M.B. Lees and J.E. Derr, A linear-Folin assay for both water-soluble and sodium dodecyl sulfate solubilised proteins, Anal. Biochem, 85 (1978) 295–300.
[15] A.R. Da Costa, Fluid Flow and Mass Transfer in Spacer-filled Channels for Ultrafiltration, Ph.D. Thesis, The University of New South Wales, Australia, 1993, Chapt. 5.
[16] J.G. Wijmans, S. Nakao, J.W.A. Van Den Berg, F.R. Troelstra and C.A. Smolders, Hydrodynamic resistance of concentration polarization boundary layers in ultrafiltration, J. Membrane Sci., 22 (1985) 117–135.
[17] A.R. Da Costa, A.G. Fane and D.E. Wiley, Ultrafiltration of whey protein solutions in spacer-filled flat channel, J. Membrane Sci., 76 (1993) 245–254.
[18] G. Jonsson, Boundary layer phenomena during ultrafiltration of dextran and whey protein solutions, Desalination, 51 (1984) 61–77.
[19] W.F. Blatt, A. Dravid, A.S. Michaels and L. Nelsen, Solute polarization and cake formation in membrane ultrafiltration: Causes, consequences and control techniques, in J.E. Flinn (Ed.), Membrane Science and Technology, Plenum Press, New York, 1970, pp. 47–97.
[20] J.P. Holman, Heat Transfer, 7th edn., McGraw Hill, New York, 1990, pp. 364–367.
[21] S.S. Kulkarni, E.W. Funk and N.N. Li, Module and process configuration, in W.S. Winston Ho and K.K. Sirkar (Eds.), Membrane Handbook, Van Nostrand Reinhold, New York, 1992, pp. 432–445.
[22] U.B. Holeschovsky and C.L. Cooney, Quantitative description of ultrafiltration in a rotating filtration device, AIChE J., 37 (1991) 1219–1226.
[23] S. Rheault and E. Bilgen, Mixed convective developing flow with reversal in open-ended inclined channels, in R.L. Mahajan et al. (Eds.), Mixed Convection and Environmental Flows, Winter Annual Meeting of ASME, Dallas, TX, 25–30 November 1990, ASME, New York, 1990, pp. 9–14.
[24] A. Acrivos, On the combined effect of forced and free convection heat transfer in laminar boundary layer flows, Chem. Eng. Sci., 21 (1966) 342–352.
[25] S.W. Churchill, A comprehensive correlating equation for laminar, assisting, forced and free convection, AIChE J., 23 (1977) 10–16.